

**MAGNETIC, SPECTRAL, THERMAL
AND STRUCTURAL PROPERTIES
OF *trans*-TETRAKIS(PYRAZOLE)BISCHLOROMANGANESE(II),
trans-HEXAKIS(PYRAZOLE)MANGANESE(II) BISPERCHLORATE
AND *trans*-TETRAKIS(PYRAZOLE)BISAQUAMANGANESE(II)
BISPYRAZOLEBISNITRATE**

PAAVO O. LUMME *, EVA LINDELL and PIRJO-RIITTA KIVIMÄKI

*Department of Inorganic Chemistry, University of Helsinki, Vuorikatu 20,
SF-00100 Helsinki (Finland)*

(Received 29 June 1987)

ABSTRACT

The complexes studied are rather unstable; their magnetic properties are in agreement with this, the paramagnetic susceptibility following the Curie–Weiss law in the temperature range 90–300 K. However, the IR spectra show M–N bands and are influenced by Hydrogen bond formation. The reflectance spectra show at least one weak band at about 23500–24200 cm^{-1} assigned to the ${}^6A_{1g} \rightarrow {}^4A_{1g}, {}^4E_g ({}^4G)$ transition. The TG curves, in agreement with the anisotropic temperature factors, coordination and hydrogen bond formation, point to differently strong-bonded pyrazole molecules in the crystal structures. The powder diffraction data of the perchlorate complex are also reported. The results are discussed and compared with previous data obtained for pyrazole complexes.

INTRODUCTION

In recent years we have reported [1–9] and performed [10] many studies on manganese(II) complexes of pyrazole (1,2-diazole). The reason for studying manganese complexes was its recently recognised biological importance [11,12]. The selection of pyrazole as the ligand was also based on its possible effectiveness in physiological processes involving manganese complexes [11,12].

In this paper we have collected magnetic, IR and reflectance spectral and thermal data for three manganese(II) complexes of pyrazole and the results are compared with earlier findings.

* Author for correspondence.

EXPERIMENTAL

*Reagents, syntheses and analyses of the compounds**trans-Tetrakis(pyrazole)bischloromanganese(II)*

This compound was prepared by dissolving $\text{MnCl}_2 \cdot 4 \text{H}_2\text{O}$ (E. Merck, p.a.) (9.9 g, 0.05 mol) and pyrazole (Fluka, purum) (3.4 g, 0.05 mol) separately in 50 ml water. The MnCl_2 solution was acidified by addition of a few drops of 0.2 M HCl. The solutions were then combined and evaporated to half volume. In 2 weeks colourless crystals separated which were filtered, washed with H_2O and dried in a desiccator. Manganese was determined by EDTA titration [13] and after cation exchange chloride was determined potentiometrically as acid with a known NaOH solution. Analysis. Found: Mn 13.81, Cl^- 17.68%, calculated for $\text{C}_{12}\text{H}_{16}\text{N}_8\text{Cl}_2\text{Mn}$: Mn 13.80, Cl^- 17.81%.

trans-Hexakis(pyrazole)manganese(II) bisperchlorate

This compound was synthesized by dissolving 3.96 g (0.02 mol) $\text{MnCl}_2 \cdot 4 \text{H}_2\text{O}$ (E. Merck, p.a.) in 20 ml hot water, followed by filtering and dropping with magnetic stirring into 40 ml hot filtered aqueous solution containing 8.17 g (0.12 mol) pyrazole (Fluka, purum), 9.79 g (0.08 mol) NaClO_4 (G.F. Smith Chemical Co.) and 4 drops 2% HCl (Merck, p.a.). Upon cooling colourless crystals were separated; they were allowed to stand for one day, then filtered on a sinter, washed with water at 5°C and dissolved in a small amount of water at 50°C with few drops of HCl. After some days colourless, prismatic crystals were separated, filtered, washed and dried in a desiccator. Metal and anion contents were determined as described above. Analysis. Found: Mn 8.32, ClO_4^- 30.05, calculated for $\text{C}_{18}\text{H}_{24}\text{N}_{12}\text{O}_8\text{Cl}_2\text{Mn}$: Mn 8.29, ClO_4^- 30.03%.

trans-Tetrakis(pyrazole)bisaquamanganese(II) bispyrazolebisnitrate

This substance was made by adding 20 ml of a filtered hot aqueous solution containing 5.02 g (0.02 mol) $\text{Mn}(\text{NO}_3)_2 \cdot 4 \text{H}_2\text{O}$ (E. Merck, p.a.) with stirring to 40 ml of a hot aqueous solution containing 8.17 g (0.12 mol) pyrazole (Fluka, purum) which had been acidified with 5 drops of 1.0 M HNO_3 (E. Merck, p.a.). The mixture was allowed to evaporate slowly and stand overnight. The separated colourless prism-shaped crystals were filtered on a sinter, recrystallized from hot water and stored in their mother liquor in a refrigerator. Dried crystals disintegrate in air. Manganese was determined as previously mentioned and nitrate was determined potentiometrically as nitric acid. Analysis. Found: Mn 8.70, NO_3^- 19.71, calculated for $\text{C}_{18}\text{H}_{28}\text{N}_{14}\text{O}_8\text{Mn}$: Mn 8.81, NO_3^- , 19.89%. The other reagents used were of guaranteed quality.

Apparatus and measurements

Magnetic susceptibility measurements of the powdered compounds (particle size 6–140 mesh) were taken on a variable-temperature Gouy balance system (Newport Instruments Ltd.) at 10 K intervals in the temperature range 93.2–303.2 K. The system was calibrated with copper(II) sulphate pentahydrate [14]. The magnetic susceptibility data are mean values from measurements on four magnetic fields. The calculated diamagnetic corrections [15,16] used were -138.3 and -316.0×10^{-6} e.m.u. for *trans*-tetrakis(pyrazole)bischloromanganese(II) and *trans*-hexakis(pyrazole)manganese(II) bisperchlorate, respectively.

Infrared spectra of KBr disks (1.5 mg compound: 200 mg KBr) were recorded on a Perkin–Elmer grating infrared spectrophotometer model 577.

Reflectance spectra were recorded on a Beckman DK-2A spectrophotometer using filter paper treated with paraffin oil paste of the compound studied.

TG curves were run on a Perkin Elmer TGS-1 thermobalance. The sample amount was 2 or 4 mg, platinum crucibles were used, the heating rate was 5, 10 or $40^\circ\text{C min}^{-1}$, and the atmosphere was either dynamic nitrogen, with a flow of about 35 ml min^{-1} , or static air.

DTA curves were run on low-temperature DTA equipment 404 T (Netzsch Gerätebau GmbH). The sample amount was 10 mg, nickel crucibles were used, the heating rate was $0.8^\circ\text{C min}^{-1}$ and the atmosphere was static air.

Powder diffraction data were obtained from photographs taken on a Guinier-Hägg camera (Philips) using 20% CaF_2 ($a = 5.4638\text{ \AA}$ [17]) as internal standard and $\text{Cu } K\alpha_1$ radiation ($\lambda = 1.5405\text{ \AA}$). Calculations were performed on a UNIVAC 1108 computer using the program PIRUM [18].

RESULTS AND DISCUSSION

Magnetic data

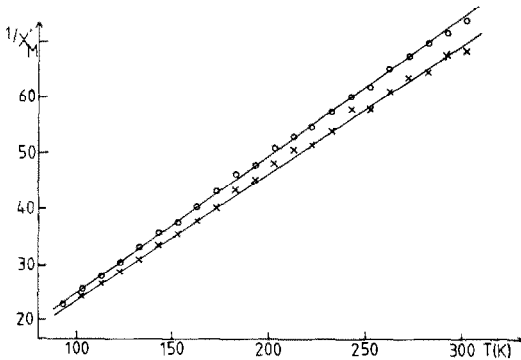
The molecular paramagnetic susceptibilities corrected for diamagnetism with Pascal's constants for the chloro and perchlorate complexes follow the Curie–Weiss law $\chi'_M = C/(T - \theta)$ between liquid nitrogen and room temperatures, i.e. between 90 and 300 K. For constant C we obtained the values 4.397(35) and 4.051(24), and for θ $-3.85(1.08)$ and $-0.37(78)$ for the chloro and perchlorate complexes, respectively. The effective magnetic moments were calculated from the equation: $\mu_{\text{eff}} = 2.83(\chi'_M \times T)^{1/2}$.

The results are presented in Table 1 and the reciprocals $1/\chi'_M$ as the function of T K in Fig. 1. The results show the manganese atoms not to have any special exchange effects in the temperature range used. This is in agreement with the weakness of the complexes. μ_{eff} is almost constant at the

TABLE 1

Magnetic data for $\text{Mn}(\text{Pz})_4(\text{Cl})_2$ and $\text{Mn}(\text{Pz})_6(\text{ClO}_4)_2$ ^a

T (K)	$\text{Mn}(\text{Pz})_4(\text{Cl})_2$			$\text{Mn}(\text{Pz})_6(\text{ClO}_4)_2$		
	μ_{eff} (B.M.)	$\chi'_M(\text{exp.})$ $\times 10^5$ (cgs e.m.u.)	$\chi'_M(\text{calcd.})$ $\times 10^5$ (cgs e.m.u.)	μ_{eff} (B.M.)	$\chi'_M(\text{exp.})$ $\times 10^5$ (cgs e.m.u.)	$\chi'_M(\text{calcd.})$ $\times 10^5$ (cgs e.m.u.)
93.2	5.790	4494	4533	5.704	4361	4332
103.2	5.824	4107	4109	5.678	3902	3913
113.2	5.852	3779	3758	5.693	3576	3569
123.2	5.880	3505	3462	5.675	3265	3280
133.2	5.880	3242	3210	5.671	3016	3034
143.2	5.848	2983	2991	5.657	2791	2823
153.2	5.888	2826	2801	5.718	2665	2639
163.2	5.883	2649	2633	5.687	2475	2477
173.2	5.880	2493	2484	5.664	2314	2335
183.2	5.824	2313	2351	5.643	2171	2207
193.2	5.861	2221	2232	5.699	2100	2093
203.2	5.818	2080	2124	5.647	1960	1990
213.2	5.813	1979	2026	5.682	1891	1897
223.2	5.901	1948	1937	5.726	1834	1812
233.2	5.884	1854	1855	5.718	1751	1735
243.2	5.812	1735	1780	5.698	1667	1664
253.2	5.937	1738	1711	5.732	1621	1598
263.2	5.879	1640	1647	5.689	1536	1537
273.2	5.868	1574	1587	5.704	1487	1481
283.2	5.936	1554	1532	5.711	1438	1429
293.2	5.906	1486	1481	5.739	1403	1380
303.2	5.969	1467	1432	5.744	1359	1335

^a Pz = $\text{C}_3\text{H}_4\text{N}_2$ (pyrazole).Fig. 1. $1/\chi'_M$ against absolute temperature T (K). Curves: \times , $\text{Mn}(\text{Pz})_4(\text{Cl})_2$; \circ , $\text{Mn}(\text{Pz})_6(\text{ClO}_4)_2$.

temperatures studied. Because of the instability of the nitrate complex its magnetic susceptibilities were not measured.

IR and reflectance spectra

In spite of their weakness the pyrazole complexes of divalent manganese ion show IR bands under 800 cm^{-1} due to manganese–nitrogen bond vibrations. This is shown in Fig. 2 for the three complexes studied and the bands of the spectra and their assignments [2] are given in Table 2. For comparison the spectrum of pyrazole is also shown in Fig. 2.

From the bands (cm^{-1}) 3400vs,br ($\nu_{\text{as}}(\text{OH}) = \nu_3(B_1)$, $\nu_s(\text{OH}) = \nu_1(A_1)$), 1620vs (HOH bending = $\nu_2(A_1)$), 1134w , 1043vw , 767vw , 570m,vbr ($\rho_r(\text{H}_2\text{O})$) shown by $\text{MnCl}_2 \cdot 4\text{H}_2\text{O}$ we can say that they are covered by the ligand bands of the chloro complex as shown in Table 2 [2,19–21]. The bands of the complex at 725 , 689 , 610 – 600 and 588 cm^{-1} are obviously due to the $\nu(\text{M-N})$ stretching vibrations.

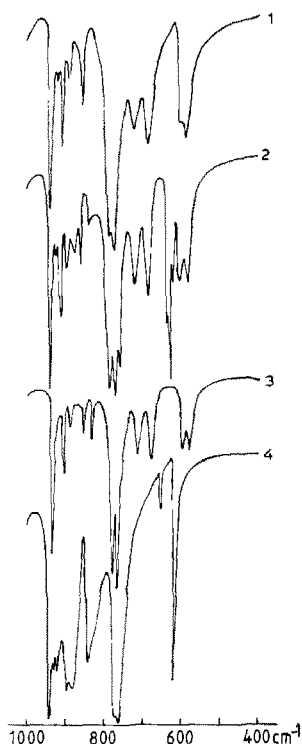


Fig. 2. Comparison of the IR spectra of the complexes and pyrazole in the wavelength range 1000 – 400 cm^{-1} . Curves: (1) $\text{Mn}(\text{Pz})_4(\text{Cl})_2$; (2) $\text{Mn}(\text{Pz})_6(\text{ClO}_4)_2$; (3) $\text{Mn}(\text{Pz})_6(\text{H}_2\text{O})_2(\text{NO}_3)_2$; (4) pyrazole.

TABLE 2

Infrared bands (cm^{-1}) of the Mn complexes and their assignments ^a

$\text{Mn}(\text{Pz})_4(\text{Cl})_2$		$\text{Mn}(\text{Pz})_6(\text{ClO}_4)_2$		$\text{Mn}(\text{Pz})_6(\text{H}_2\text{O})_2(\text{NO}_3)_2$		Assignment
3360–3300	vs	3340–3290	vs	3340–3280	vs	$\nu(\text{NH})$
3136	m	3160–3110	s	3130	vw	$\nu(\text{CH})$
3115	m			3100	m	$\nu(\text{CH})$
		3050–2810	m	2418	m	c. and o.
1750–1740	w	1750	vw			$\nu(\text{ring})$
1625–1620	w	1625	w			$\nu(\text{ring}), \nu(\text{ClO}_4^-)$
1518	s	1518	s	1520	m	$\delta(\text{ring})$
1469	vs	1468	vs	1460	m	$\delta(\text{ring})$
1459	s	1460	s	1458	s	$\delta(\text{ring})$
1400	s	1400	vs	1380–1370	vs	$\delta(\text{ring}), \nu(\text{ClO}_4^-)$
1350	vs	1350	vs	1345	s	$\delta(\text{ring})$
1256	m	1257	m	1255	m	$\delta(\text{CH})$
1158	s	1160–1080	vs	1150	m	$\delta(\text{NH}), \nu(\text{ClO}_4^-)$
1128	vs			1120	s	$\delta(\text{NH})$
1118	vs			1110	s	$\delta(\text{NH})$
1065	vs	1065	vs	1058	s	$\delta(\text{CH})$
1055	vs	1057	w			$\delta(\text{CH})$
1045	vs	1045	vs	1038	vs	$\delta(\text{CH})$
942	vs	942	vs	935	vs	$\delta(\text{ring}), \nu(\text{ClO}_4^-)$
922	m	927	w			$\delta(\text{ring})$
912	s	914	s	905	m	$\delta(\text{ring})$
894	m	897	m	890	w	$\delta(\text{CH})$
861	m	862	m	854, 832	m	$\delta(\text{CH})$
789	vs	788	vs	780	vs	$\delta(\text{CH})$
776	vs	774, 762	vs	768	vs	$\delta(\text{CH})$
725	s	720	s	712	m	$\nu(\text{M-X}),$ X = N, O, Cl
689	s	687	s	678	m	$\nu(\text{M-N})$
		640, 630, 621	vs			$\nu(\text{ClO}_4^-)$
610–600	s	605	s	597	m	$\nu(\text{M-N})$
588	s	584	s	578	m	$\nu(\text{M-N})$

^a Abbreviations: b, broad; m, medium; s, strong; v, very; w, weak; ν , stretching; δ , bending; c., combination; o., overtones.

Generally in the spectra of all three complexes the band at 3150–3100 cm^{-1} is due to C–H stretching vibrations of the pyrazole molecules. The strong, medium or weak bands in the 3050–762 cm^{-1} range are assigned to combination and overtone bands or stretching and deformation bands of the pyrazole ring with individual overlaps as pointed out in Table 2.

The weak and broad bands at 2025, 475 and 405 cm^{-1} shown by NaClO_4 have disappeared from the spectrum of the perchlorate complex. Instead, the bands (cm^{-1}) 1625w, 1400s, 1160–1180vs,br, 942s, 640vs and 630vs due to ClO_4 vibrations in the spectrum of NaClO_4 are partly, at least, under the

bands at the same regions in the spectrum of the perchlorate complex. This complex also obviously shows $\nu(\text{M-N})$ bands at 720vs, 687s, 605s and 584s cm^{-1} .

The very strong and broad band at 3400–3300 cm^{-1} in the spectrum of the nitrate complex is due to three kinds of vibrations ($\nu_1(A_1, \text{OH})$, $\nu(\text{NH})$ and $\nu_3(B_1, \text{NO})$) which overlap each other [2,19–21]. The strong band at 1610 cm^{-1} observed in the spectrum of manganese dinitrate tetrahydrate and due to overlapping of OH bending ($\nu_2(A_1)$ and NO_3 ($\nu_3(\text{NO}_3)$)) stretching vibrations is missing from the complex spectrum. This must be due to hydrogen bond formation in the crystals [3,10]. The strong and broad band at 1380–1370 cm^{-1} is due to pyrazole ring deformation and $\text{NO}(A_1)$ stretching vibrations. Manganese dinitrate tetrahydrate shows a very strong band at 1370 cm^{-1} . Further it shows a weak NO stretching ($\nu_1(\text{NO}_3, A_1)$) band at 1040 cm^{-1} and a medium 840 cm^{-1} band due to overlapping H_2O rocking ($\rho_r(\text{H}_2\text{O})$) and NO_3 stretching ($\nu_2(\text{NO}_3)$) vibrations. These bands are overlapped in the complex spectrum and obviously again this is due to hydrogen bond formation.

In general the medium strong bands below 750 cm^{-1} are assigned to Mn–N stretching bands due to pyrazole coordination to the manganese(II) ion in the complexes.

The bands (cm^{-1}) of the reflectance spectra of the complexes studied with their assignments are presented in Table 3. The bands in the area 10000–8000 cm^{-1} are assigned to the pyrazole ligand. The weak bands at 25000–23000 cm^{-1} are assigned to the electron transitions ${}^6A_{1g} \rightarrow {}^4A_{1g}$, ${}^4E_g({}^4G)$ at the manganese(II) ion [22,23]. The bands at 28000 cm^{-1} are correspondingly assigned to ${}^6A_{1g} \rightarrow {}^4T_{2g}({}^4G)$ transitions at the metal ions. The weakness or disappearance of the reflectance bands due to complex formation is in accordance with the weakness of the complexes.

TG and DTA data

The results of the thermal analyses of the complexes are presented in Tables 4–6 and in Fig. 3. In Table 4 the TG and DTA data, obtained in a static air atmosphere, are compared for the chloro complex. Pyrazole molecules escape successively from the complex, loss occurring in the temperature ranges 170–240, 240–270 and 270–380 °C. The manganese(II) chloride

TABLE 3

Bands (cm^{-1}) of the reflectance spectra of the Mn complexes and their assignments

$\text{Mn}(\text{Pz})_4(\text{Cl})_2$	$\text{Mn}(\text{Pz})_6(\text{ClO}_4)_2$	$\text{Mn}(\text{Pz})_6(\text{H}_2\text{O})_2(\text{NO}_3)_2$	Assignment
28090			${}^6A_{1g} \rightarrow {}^4T_{2g}({}^4G)$
23585	23980	23800	${}^6A_{1g} \rightarrow {}^4A_{1g}$, ${}^4E_g({}^4G)$
8330	9800, 9090, 8330	9640, 9090, 8330	Pyrazole

TABLE 4

TG and DTA data for $\text{Mn}(\text{Pz})_4(\text{Cl})_2$

Process	TG ^a		DTA		
	Temp. range (°C)	Residue (%)		Peak temp. (°C)	Peak nature
		Found	Calcd.		
$\text{Mn}(\text{Pz})_4(\text{Cl})_2$	170–240	67.6	65.8	150, 190	Endo
↓					
$\text{Mn}(\text{Pz})_2(\text{Cl})_2$	240–270	50.1	48.7	260	Endo
↓					
$\text{Mn}(\text{Pz})(\text{Cl})_2$	270–380	32.6	31.6	300	Endo
↓					
MnCl_2	510–770	20.2	19.8	400	Endo
↓					
Mn_2O_3	> 770				

^a The heating rate was $40^\circ\text{C min}^{-1}$ in a static air atmosphere.

remaining is oxidized at $510\text{--}770^\circ\text{C}$ to Mn_2O_3 . The first DTA peak (150°C) corresponds to melting of the complex and the others correspond roughly to the processes indicated by the TG curve. All processes are endothermic.

The effect of the heating rate on thermal stability and its reproducibility in the case of the perchlorate complex in a dynamic nitrogen atmosphere are represented in Table 5 (Fig. 3). At the lower heating rate the pyrazole molecules escape in four steps: one and a half, a half, two and two in the temperature ranges $175\text{--}222$, $222\text{--}255$, $255\text{--}285$ and $285\text{--}324^\circ\text{C}$, respectively. The manganese(II) perchlorate remaining explodes at $324\text{--}330^\circ\text{C}$. Increasing the heating rate from 5 to $10^\circ\text{C min}^{-1}$ accelerates the decomposition process; the pyrazole molecules escape in three steps, and the temperature ranges are raised somewhat. In a static air atmosphere, however, the TG curves [7] of the perchlorate complex were similar at the 5 and $10^\circ\text{C min}^{-1}$ heating rates.

The effect of the atmosphere (static air or dynamic nitrogen) on the thermal stability of the nitrate complex is elucidated in Table 6. The atmosphere seems not to affect the decomposition order, but the dynamic N_2 atmosphere mostly increases and expands the decomposition temperature ranges as compared with those in the static air atmosphere. The complex firstly gives up both H_2O and one pyrazole molecule, then three pyrazoles and lastly decomposes directly to impure Mn_2O_3 .

The present results in the dynamic N_2 atmosphere differ from those obtained earlier [7] with a heating rate of $10^\circ\text{C min}^{-1}$; there the TG curve showed the mono pyrazole complex to be the last step before the residue.

Generally the decomposition reactions of the title complexes follow a pattern in which the ligand molecules escape in steps according to the

TABLE 5

TG data for $\text{Mn}(\text{Pz})_6(\text{ClO}_4)_2$ ^a

Process	TG(5°C min ⁻¹) ^b		TG(10°C min ⁻¹) ^c		TG(10°C min ⁻¹) ^b	
	Temp. range (°C)	Residue (%)	Temp. range (°C)	Residue (%)	Temp. range (°C)	Residue (%)
		Found		Calcd.		Found
$\text{Mn}(\text{Pz})_6(\text{ClO}_4)_2$						
↓	175–222	83.0	185–248	82.9	180–238	83.5
$\text{Mn}(\text{Pz})_{4.5}(\text{ClO}_4)_2$						
↓	222–255	77.1	248–285	74.8	238–305	
$\text{Mn}(\text{Pz})_4(\text{ClO}_4)_2$						
↓	255–285	60.6	285–378			59.2
$\text{Mn}(\text{Pz})_2(\text{ClO}_4)_2$						
↓	285–324	34.4		40.3	305–370	25.2
$\text{Mn}(\text{ClO}_4)_2$						
↓	324–330	2.9	> 378		370–375	7.1
Mn_2O_3	> 330				> 375	

^a Dynamic N₂ atmosphere. ^b 2 mg sample. ^c 4 mg sample.

TABLE 6

TG data for $\text{Mn}(\text{Pz})_6(\text{H}_2\text{O})_2(\text{NO}_3)_2$ ^a

Process	TG(N ₂) ^b		TG(static air) ^c		
	Temp. range (°C)	Residue (%)		Temp. range (°C)	Residue (%)
		Found	Calcd.		Found
$\text{Mn}(\text{Pz})_6(\text{H}_2\text{O})_2(\text{NO}_3)_2$	45–127			63–116	
↓ $\text{Mn}(\text{Pz})_5(\text{NO}_3)_2$	127–213	81.0	83.3	116–200	81.8
↓ $\text{Mn}(\text{Pz})_2(\text{NO}_3)_2$	213–494	46.3	50.5	200–365	50.8
↓ Mn_2O_3 (impure)	> 494	14.5	12.7	> 365	22.0

^a Heating rate 5 °C min⁻¹. ^b 4 mg sample. ^c 2 mg sample.

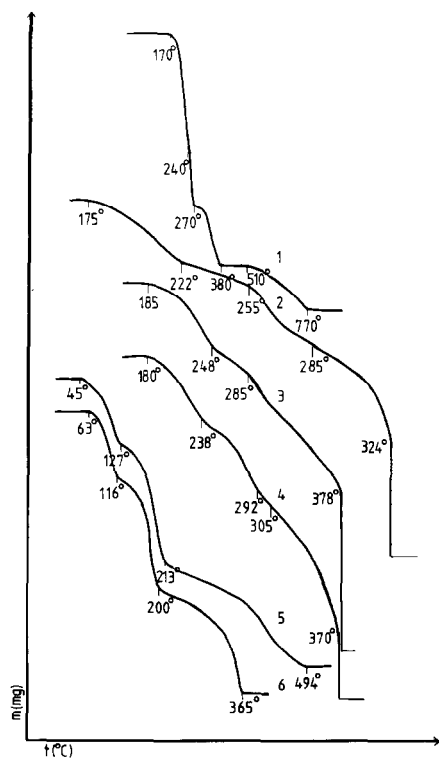


Fig. 3. TG curves of the Mn complexes in dynamic nitrogen or static air atmosphere. Curves: (1) $\text{Mn}(\text{Pz})_4(\text{Cl})_2$, static air, 40 °C min⁻¹; (2) $\text{Mn}(\text{Pz})_6(\text{ClO}_4)_2$, dynamic nitrogen, 5 °C min⁻¹; (3) $\text{Mn}(\text{Pz})_6(\text{ClO}_4)_2$, dynamic nitrogen, 10 °C min⁻¹; (4) $\text{Mn}(\text{Pz})_6(\text{ClO}_4)_2$, dynamic nitrogen, 10 °C min⁻¹; (5) $\text{Mn}(\text{Pz})_6(\text{H}_2\text{O})_2(\text{NO}_3)_2$, dynamic nitrogen, 5 °C min⁻¹; (6) $\text{Mn}(\text{Pz})_6(\text{H}_2\text{O})_2(\text{NO}_3)_2$, static air, 5 °C min⁻¹. For the sample amounts used see Tables 4–6 and the Experimental section.

TABLE 7

Observed and calculated d spacings (Å) and estimated relative intensities of the powder lines for $\text{Mn}(\text{Pz})_6(\text{ClO}_4)_2$

hkl	d_o	d_c	I/I_o^a	hkl	d_o	d_c	I/I_o^a
100	8.752	8.740	w	210	3.302	3.303	vw
001	8.020	8.010	s	112	3.139	3.137	w
101	5.909	5.905	m	202	2.953	2.953	vw
110	5.047	5.046	m	300	2.913	2.913	vw
200	4.369	4.370	w	301	2.737	2.738	w
111	4.271	4.269	s	212	2.548	2.548	m
002	4.006	4.005	vw	311	2.322	2.320	w
201	3.838	3.836	vs	213	2.076	2.077	w
102	3.644	3.641	w				

^a Abbreviations: m, medium; s, strong; v, very; w, weak.

strength of their bonding to the central metal atom and in agreement with the values of the anisotropic temperature factors [1–10].

Structural data

Preliminary reports of the crystal structures of the complexes studied have been presented previously [3–5] and will be published in full elsewhere [10]. The powder diffraction data of *trans*-tetrakis(pyrazole)bis(isothiocyanato)manganese(II), which crystallized in the monoclinic space group $C2/c$ with $Z = 4$, have been published [2]. For comparison we report in Table 7 the d spacings for *trans*-hexakis(pyrazole)manganese(II) bisperchlorate, which crystallized in the trigonal space group $P\bar{3}$ with $Z = 1$. For unit cell dimensions we obtained $a = 10.092(3)$ and $c = 8.010(2)$ Å, $V = 706(32)$ Å³. These are comparable with the four-circle diffractometer data [4,10]: $a = 10.129(4)$, $c = 8.039(5)$ Å, and $V = 714.3(6)$ Å³.

CONCLUSION

Generally the mixed pyrazole complexes of divalent manganese ion show variable compositions and crystal symmetry. Some have a hydrogen bond net stabilizing the crystal structure, but in some only van der Waals forces are effective. The thermal, magnetic and reflectance spectral properties are in accord with structures and the weakness of the complexes. The IR spectra, however, imply in every case metal–nitrogen coordination.

ACKNOWLEDGEMENT

Financial support from the Academy of Finland (Suomen Akatemia) is gratefully acknowledged.

REFERENCES

- 1 P. Lumme, I. Mutikainen and E. Lindell, Abstr. 7th Eur. Crystallogr. Meet., Jerusalem, Israel, 1982, p. 148.
- 2 P. Lumme, I. Mutikainen and E. Lindell, *Inorg. Chim. Acta*, 71 (1983) 217.
- 3 P. Lumme, E. Lindell and I. Mutikainen, Abstr. 8th Eur. Crystallogr. Meet., Liège, Belgium, 1983, Imprimerie C.L.R.O., Liège, p. 129.
- 4 P.O. Lumme, E. Lindell and I. Mutikainen, Abstr. XI Nordiske Strukturkjemikermøte, Tromsø, Norway, 1984, p. 61.
- 5 P.O. Lumme, E. Lindell and P.-R. Kivimäki, Abstr. XI Nordiske Strukturkjemikermøte, Tromsø, Norway, 1984, p. 33.
- 6 P.O. Lumme, Abstr. 3rd Eur. Symp. Thermal Analysis and Calorimetry, Interlaken, Switzerland, 1984, p. C 75.
- 7 P.O. Lumme, *Thermochim. Acta*, 86 (1985) 101.
- 8 P. Lumme and E. Lindell, Abstr. 9th Eur. Crystallographic Meet., Torino, Italy, 1985, Vol. I, p. 201.
- 9 P. Lumme and E. Lindell, *J. Coord. Chem.*, 15 (1986) 383.
- 10 P. Lumme, E. Lindell and I. Mutikainen, unpublished results.
- 11 H. Sigel (Ed.), *Metal Ions in Biological Systems*, Vols. 3 (1974), 6 (1976), 8–10 (1979–80), 12–15 (1981–83), Marcel Dekker, New York.
- 12 D.W. Martin, Jr., P.A. Mayes and V.W. Rodwell (Eds.), *Harper's Review of Biochemistry*, Lange, Los Altos, California, 1983.
- 13 A.I. Vogel, *Quantitative Inorganic Analysis*, 3rd Edn., Longmans, London, 1961, p. 434.
- 14 B.N. Figgis and J. Lewis, in H.B. Jonassen and A. Weissberger (Eds.), *Technique of Inorganic Chemistry*, Vol. 4, Interscience, London, 1965, p. 231.
- 15 A. Weiss and H. Witte, *Magnetochemie, Grundlagen und Anwendungen*, Verlag Chemie, Weinheim, 1973, p. 95.
- 16 A. Earnshaw, *Introduction to Magnetochemistry*, Academic Press, London, 1968, pp. 4–8.
- 17 D.N. Batchelder and R.O. Simmons, *J. Chem. Phys.*, 41 (1964) 2324.
- 18 P.E. Werner, *J. Appl. Crystallogr.*, 9 (1976) 216.
- 19 H. Siebert, *Anwendungen der Schwingungsspektroskopie in der anorganischen Chemie*, Springer-Verlag, Berlin, 1966, pp. 43, 68, 91, 104, 143–45, 148.
- 20 K. Nakamoto, *Infrared and Raman Spectra of Inorganic and Coordination Compounds*, 4th Edn., Wiley, New York, 1986, pp. 115, 124, 191–197, 228–230, 251, 253–257, 324–329.
- 21 A. Zecchina, L. Cerruti, S. Coluccia and E. Borello, *J. Chem. Soc. B*, (1967) 1363.
- 22 H.L. Schläfer and G. Gliemann, *Einführung in die Ligandenfeldtheorie*, Akademische Verlagsgesellschaft, Frankfurt am Main, 1967, pp. 52, 98.
- 23 A.B.P. Lever, *Inorganic Electronic Spectroscopy*, Elsevier, Amsterdam, 1968, p. 292.